Investigation of Methyl-5-(pentan-3-yloxy)-7-oxabicyclo[4.1.0]hept-3-ene-3-carboxyhydrazide Derivatives as Potential Inhibitors of COVID-19 Main Protease: DFT and Molecular Docking Study

Bioinformatics and Biology Insights
Volume 17: 1–12
© The Author(s) 2023
Article reuse guidelines:
sagepub.com/journals-permissions
DOI: 10.1177/11779322231182050

Olawale Folorunso Akinyele[1], Emmanuel Gabriel Fakola[1], Omolara Olubunmi Adeboye[2] and Sunday Chimela Chinuomah[1]

[1]Department of Chemistry, Obafemi Awolowo University, Ile-Ife, Nigeria. [2]Department of Chemistry, Emmanuel Alayande College of Education, Oyo, Nigeria.

ABSTRACT: The search for effective therapeutics to combat COVID-19 has led to the exploration of the biological activity of numerous compounds. In this study, hydrazones derived from oseltamivir intermediate, methyl 5-(pentan-3-yloxy)-7-oxabicyclo[4.1.0]hept-3-ene-3-carboxylate have been investigated for their potential as drug candidates against the COVID-19 virus using computational methods, including density functional theory (DFT) studies, molecular docking, and absorption, distribution, metabolism, excretion and toxicity (ADMET) analysis. The DFT studies provide information on the electronic properties of the compounds while the molecular docking results using AutoDock reported the binding energies between the main protease of COVID-19 and the compounds. The DFT results revealed that the energy gap of the compounds ranged from 4.32 to 5.82 eV while compound HC had the highest energy gap (5.82 eV) and chemical potential (2.90 eV). The electrophilicity index values of the 11 compounds ranged from 2.49 to 3.86, thus they were classified as strong electrophiles. The molecular electrostatic potential (MESP) revealed electron-rich and electron-deficient regions of the compounds. The docking results reveal that all the compounds had better docking scores than remdesivir and chloroquine, frontline drugs employed in combating COVID-19, with HC having the best docking score of -6.5. The results were visualized using Discovery studio, which revealed hydrogen bonding, pi-alkyl interaction, alkyl interaction, salt bridge interaction, halogen interaction as being responsible for the docking scores. The drug-likeness results showed that the compounds qualify as oral drug candidates as none of them violated Vebers and Lipinski's rule. Thus, they could serve as potential inhibitors of COVID-19.

KEYWORDS: Hydrazones, main protease inhibitors, oseltamivir, density functional theory, molecular docking

RECEIVED: January 31, 2023. **ACCEPTED:** May 27, 2023.

TYPE: Original Research Article

FUNDING: The author(s) received no financial support for the research, authorship, and/or publication of this article.

DECLARATION OF CONFLICTING INTERESTS: The author(s) declared no potential conflicts of interest with respect to the research, authorship, and/or publication of this article.

CORRESPONDING AUTHOR: Emmanuel Gabriel Fakola, Department of Chemistry, Obafemi Awolowo University, Ile-Ife, Osun State, Nigeria. Email: emmseg98@yahoo.com

Introduction

The persistence of the COVID-19 pandemic for over 24 months is a crucial issue, especially as it still causes death, respiratory issues, and affects the world's economy. The pandemic caused by a virus (severe acute respiratory syndrome corona virus [SARS-CoV-2]), which belongs to the family β-*Coronaviridae*, as of March 29, 2023, has led to the death of 6.8 million individuals with more than 761 million cases of COVID-19 reported globally.[1,2] Considering the debilitating effect of the pandemic, numerous studies have been carried out to develop effective antiviral agents against SARS-CoV-2.

Among the potential targets for antiviral drugs, viral proteases have received considerable attention. Proteases have proven effective in combating diseases such as HIV, Ebola, and Hepatitis C.[3] Studies have unveiled the crucial role of the main protease (Mpro) in the replication of SARS-CoV-2.[4-6] Mpro plays a vital role in activating functional and non-structural proteins necessary for viral replication. By cleaving viral polyproteins at specific sites, Mpro releases individual viral proteins required for replication and assembly of new viral particles.[7,8] Due to its significance in the viral life cycle, Mpro has become a primary target for drug development to treat COVID-19. Inhibiting Mpro's activity with small molecule inhibitors or other therapeutic agents has the potential to disrupt viral replication and mitigate the severity of COVID-19 symptoms.[9-11]

To gain insight into the interaction between a ligand and a protein, particularly in drug discovery, molecular docking is employed.[12,13] It provides valuable predictions regarding the most probable binding mode of a compound with a protein.[14] Combined with ADMET properties, molecular docking can offer useful insights into the drug-like properties of compounds and the biochemical pathways and molecular mechanisms of drug-protein interactions.[15-18] In addition, density functional theory (DFT) studies have been used to investigate the selectivity, reactivity, and electronic effects of ligands and potential drug candidates.[19,20] This technique plays a crucial role in understanding ligand properties, reaction mechanisms, and predicting experimental phenomena, thus contributing to drug discovery efforts.[21]

Hydrazones which are synthetically produced by the reaction between hydrazides and carbonyl compounds have shown interesting properties and versatile behaviour.[22] Hydrazones are azomethines containing a triatomic group >C=N–N<. They differ from other members of this class (the imines and oximes) by the presence of two interlinked nitrogen atoms.[23] Hydrazones have a wide application as they are employed in

Creative Commons Non Commercial CC BY-NC: This article is distributed under the terms of the Creative Commons Attribution-NonCommercial 4.0 License (https://creativecommons.org/licenses/by-nc/4.0/) which permits non-commercial use, reproduction and distribution of the work without further permission provided the original work is attributed as specified on the SAGE and Open Access pages (https://us.sagepub.com/en-us/nam/open-access-at-sage).

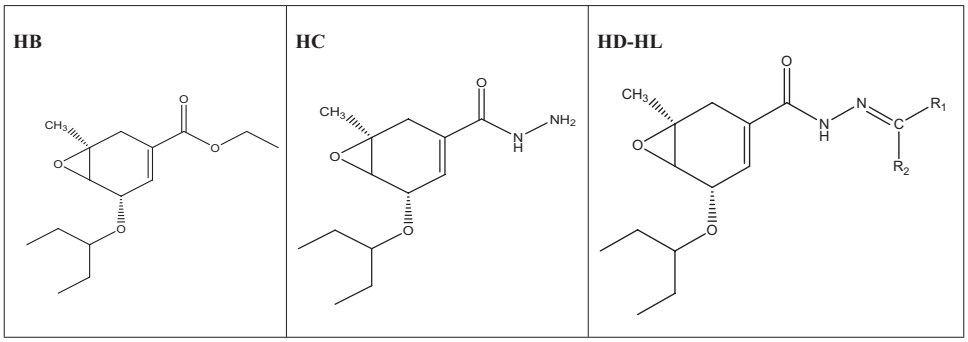

Figure 1. Structure of (1S,5S)-ethyl 1-methyl-5-(pentan-3-yloxy)-7-oxabicyclo[4.1.0]hept-3-ene-3-carboxylate (HB), (1S,5S)-ethyl 1-methyl-5-(pentan-3-yloxy)-7-oxabicyclo[4.1.0]hept-3-ene-3-carboxhydrazide (HC) and corresponding hydrazones (HD-HL).
HD–R_1 = H, R_2 = C_6H_5; **HE**–R_1 = H, R_2 = $C_6H_3(OCH_3)(OH)$; **HF**–R_1 = CH_3, R_2 = C_6H_5.
HG–R_1 = H, R_2 = $C_6H_3(OCH_3)(CH_3)$; **HH**–R_1 = H, R_2 = C_6H_4N; **HI**–R_1 = CH_3, R_2 = C_6H_4N.
HJ–R_1 = H, R_2 = $C_6H_3(OCH_3)(Cl)$; **HK**- R_1 = H, R_2 = $C_6H_4(OCH_3)$; **HL**–R_1 = H, R_2 = $C_6H_3(OCH_3)(F)$.

drug design, coordination chemistry, catalysis, and the synthetic formation of heterocyclic compounds. Hydrazones have been extensively studied for a long time due to their desirable characteristics, which include ease of preparation, increased hydrolytic stability in relation to imines and the tendency to form crystals.[24] Several hydrazides and hydrazones are used as drugs, while some have been reported to possess drug-like and medicinal properties such as antioxidant, anticancer, antibacterial, and antiviral activities.[25,26] These properties have sparked an interest in the further exploration of hydrazones as effective antiviral agents for tackling COVID-19.

Ostelamivir is a neuraminidase inhibitor. It was approved in 1999 by the US Food and Drug Administration (FDA) and is employed in treating influenza A and B.[27] Oseltamivir was first linked to the coronavirus during the break out of atypical pneumonia caused by acute respiratory syndrome. A study showed that the active site of the spike 1 protein of SARS resembles that of neuraminidase. This suggests that inhibitors of neuraminidase might be effective in treating SARS-CoV-2. Although no clinical data are yet to establish the effectiveness of oseltamivir towards coronaviruses, studies have shown that hydrazone derivatives of compounds can possess interesting inhibitory activities towards coronaviruses especially as oseltamivir is used to treat viral-related issues.[28,29]

Hydrazones are a highly versatile chemical moiety that can be modified in a number of ways to produce analogs with improved pharmacological properties.[30] The presence of the hydrazone functional group allows for the formation of various types of covalent and non-covalent interactions with target biomolecules, such as enzymes and receptors, which can lead to the modulation of their activity.[31] This is of great interest in combating COVID-19, given that one of the key challenges in developing drugs against COVID-19 is the high rate of mutation of the SARS-CoV-2 virus, which can lead to the emergence of new variants that may be more resistant to existing treatments.[32,33]

The ease with which hydrazones can be synthesized and modified makes them an attractive target for drug development. Various substitutions on the aromatic or aliphatic rings of the hydrazones can significantly alter their physicochemical properties, such as lipophilicity, solubility, and bioavailability, which can affect their pharmacokinetic and pharmacodynamic properties.[26] Moreover, hydrazones can also be modified by introducing additional functional groups, such as carbonyl, ester, and amide groups, onto the hydrazone moiety.[34] These modifications can enhance the metabolic stability, water solubility, and permeability of the drug, which can improve its pharmacokinetic properties.[35,36] The interesting properties of hydrazones makes them significant in the development of effective drugs against COVID-19. However, there is a paucity of data regarding the examination of hydrazones as effective therapeutic agents against COVID-19 in the literature. Therefore, this study aims to investigate the inhibitory activity of hydrazides and hydrazones derived from oseltamivir intermediate, methyl 5-(pentan-3-yloxy)-7-oxabicyclo[4.1.0]hept-3-ene-3-carboxylate, towards the main protease of SARS-COV-2 and explore their electronic properties. The structures of the oseltamivir intermediate and its carboxyhydrazide derivatives are shown in Figure 1.

Chemistry

The proposed method for the synthesis of the compounds is thus:

(a) The derivative of oseltamivir intermediate undergoes a condensation reaction to form a hydrazide.

(b) The hydrazide undergoes a condensation reaction with aldehyde and ketones to form hydrazones.

The structure of oseltamivir is shown in Figure 2, while the scheme of the reaction is shown in Figure 3.

Experimental

DFT calculations

In this study, we employed DFT, an advanced theoretical chemistry approach, to investigate the physicochemical properties of

the compounds. Prior to DFT quantum calculations, we first conducted a conformer distribution examination on each of the compounds using B3LYP hybrid functional methods with the 6–31G* basis set implemented in Spartan 14 computational software.[37] We used the most stable conformer for subsequent calculations, which was carried out on an HP 2000 Notebook computer with an Intel® Core™ i3-3120M CPU @ 2.50 GHz, 296 GB SSD, and 4.00 GB RAM. Our calculations included determining the frontier molecular orbital energies, highest occupied molecular orbital energy (E_{HOMO}), and lowest unoccupied molecular orbital energy (E_{LUMO}). These calculations were carried out on the gas phase. Quantum parameters such as ionization energy (I), electron affinity (A), chemical hardness (η), electronic chemical potential (μ), and electronegativity (χ) were computed from the frontier molecular orbital energies using the following relationships as presented in Equations (1) to (7).[37-40]

$$\text{Energy gap}\left(E_g\right) = E_{LUMO} - E_{HOMO} \quad (1)$$

$$\text{Ionisation energy}\left(I\right) = -E_{HOMO} \quad (2)$$

$$\text{Electroaffinity}\left(A\right) = -E_{LUMO} \quad (3)$$

$$\text{Electronegativity}\left(\chi\right) = -\eta \quad (4)$$

$$\text{Chemical hardness}\left(\eta\right) = \frac{1}{2}\left(E_{LUMO} - E_{HOMO}\right) \quad (5)$$

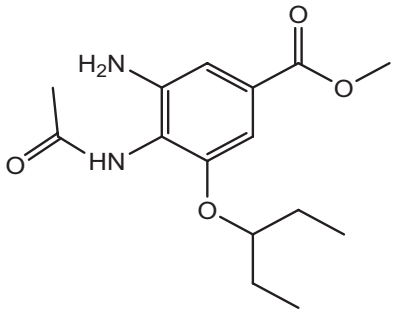

Figure 2. Structure of oseltamivir.

$$\text{Chemical potential}\left(\mu\right) = \frac{1}{2}\left(E_{HOMO} + E_{LUMO}\right) \quad (6)$$

$$\text{Electrophilicity index}\left(\omega\right) = \frac{\mu^2}{2\eta} \quad (7)$$

The B3LYP method was used to optimize all of the structures, and the molecular electrostatic potential (MESP) analysis was generated using Spartan 14 software.[41,42]

Drug-likeness

To predict the drug-likeness properties of the selected compounds, insilico adsorption, distribution, metabolism, excretion, and toxicity test was carried out using the Swiss ADME (http://www.swissadme.ch/).[43] Important drug-like parameters such as octanol-water partition coefficient (Log P), molecular weight, number of hydrogen bond acceptors and hydrogen bond donors, molecular surface area (PSA), violations to the Lipinksi rule, and Veber rules were computed.

Molecular docking

The three-dimensional (3D) crystal structure of the main protease (Mpro) with PDB 6LU7 was obtained from the protein data bank. In the docking study, the protein (PDB 6LU7) was considered rigid. Protein preparation involved using the Pymol software to remove water molecules, ions, cofactors, and co-crystallized ligands. In addition, charges and hydrogen were added to the protein using the MGL tool 1.5.2. To validate the docking protocol, the co-crystallized ligand was re-docked into the binding pocket of 6LU7 using PyRx 0.840, and the RMSD value between the co-crystallized ligand and the re-docked ligand was computed.[40]

Ligand modelling. A total of 10 hydrazones and 1 hydrazide were generated using ChemDraw software, and their 3D structures were obtained using Chem-3D. The ligand structures underwent energy minimization using the MMF94x force field in the PyRx 0.8 tool, specifically the Open Babel plugin

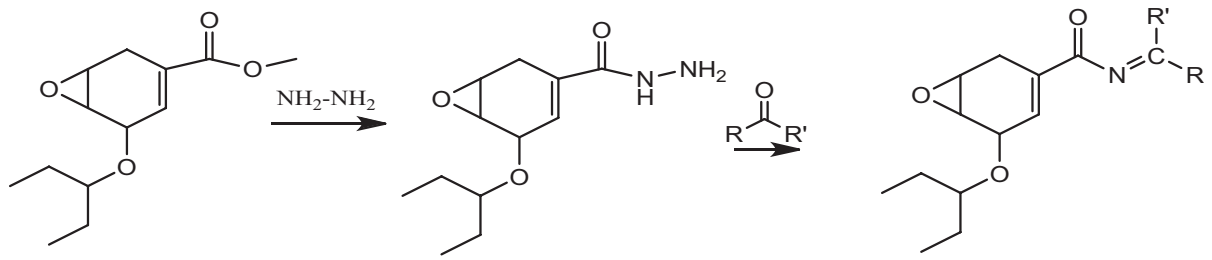

Figure 3. Synthetic route for hydrazide and hydrazones of oseltamivir intermediate derivative.

Table 1. Docking scores of the compounds and interacting amino acids.

COMPOUNDS	DOCKING SCORE	INTERACTING AMINO ACIDS
HB	−5.3	ILE106, ASP 153
HC	−6.5	GLN 110, THR111, ASN151, THR292, PHE294
HD	−5.8	ASN151, VAL 104
HE	−6.0	ASN151, ASP153, PHE 294
HF	−6.1	GLN 110, VAL104, ASN151
HG	−5.9	PHE294, VAL104, ASN 151, THR111
HH	−5.6	GLN 110, ASN151, THR292, PHE294, ASP 153, ILE152, VAL 104
HI	−6.1	GLN 110, PHE294, ASP 153, ILE152, VAL 104, SER 158
HJ	−5.9	PHE 294, ASP 153, SER 158, VAL 104
HK	−5.9	VAL104, ARG, ASN 151, ASP153
Chloroquine	−5.2	PHE 294
Remdesivir	−5.4	GLY 138, LYS 137

tool and were subsequently saved in PDB format for subsequent docking analyses.[40]

To carry out molecular docking, the energy of the compounds was minimized under MMFF94x force field employing the steepest descent method for 200 steps with a step size of 0.02 and converted from PDB open babel programme in PyRx 0.8 software. Next, the grid box size was set at 25 Å and centre at X = −25.9959 Å, Y = 12.5892 Å, and Z = 59.1535 Å for the main protease (Mpro). Molecular docking was performed to exhaustiveness of 50 using the AutoDock Vina tool in PyRx 0.8.37. Results were obtained with the lowest RMSD value and best binding energy. Later on, interactions like hydrogen bond, hydrophobic, and pi were chosen and analysed using Discovery studio visualizer 2020.

Results and Discussion

Molecular docking

The docking results for the 11 compounds reveal that the binding affinity for the compounds ranges from −5.3 to −6.5. The binding affinity follows the trend HC > HF > HI > HE > HG > HJ > HK > HL > HD > HH > HB. Several interactions were responsible for the docking results. These interactions included hydrogen bonding, pi-alkyl interaction, alkyl interaction, salt bridge interaction, halogen interaction, and other interactions. All of the compounds except HB had better docking scores than remdesivir and chloroquine, frontline drug candidates for combating COVID-19. HB interacts with the protein via a carbon hydrogen bond with ASP 153 and an alkyl bond with ILE106. HC with the best docking score formed hydrogen bonds with GLN 110, THR 111, ASN 151, and THR 292. It also interacted with ASP 295 and PHE 294 via a salt bridge and a pi-alkyl bond respectively. HD and HE like HC interacted with ASN 151 via a hydrogen bond. However, HD interacted with VAL 104 through an alkyl bond while HE interacted with PHE 294 through a pi-alkyl bond. Two hydrogen bonds between HF and ASN 151 and GLN 110 as well as alkyl interaction were responsible for its relatively high docking. HG interacts with PHE 294 and VAL 104 through a pi-sigma bond and pi-alkyl bond respectively. HH interacts with ASN 151 and THR 111 via hydrogen bonds. It interacts with PHE 294 and VAL 104 via a pi-sigma and alkyl bond. HI bond to GLN 110, SER 158 and ILE 152 through hydrogen bonds. In addition, HI interact with ASP 153, VAL 104 and PHE 294 through a pi-anion, alkyl and pi-pi stacked interaction. HJ interacts with SER158 through a hydrogen bond and interacts with PHE 294 and VAL 104 through a pi-alkyl interaction. HK interacted with ASN 151 via a hydrogen bond, with VAL 104 through an alkyl interaction and ASP 153 through an attractive charge interaction. HL interacted with ASN 151 through a hydrogen bond. It also interacted with PHE 294 through a pi-sigma interaction. Furthermore, it interacted with ILE 106 and ARG 105 through halogen interaction. These interactions are listed and shown in Table 1. The visualizations of the interaction are shown in Figure 4.

The findings of this study align with previous research conducted by Indu et al. in 2020. The antiviral compounds assessed in that study: raltegravir, indinavir, tipranavir, dolutegravir, and etravirine interacted with amino acids such as VAL 104, ARG 105, ILE 106, GLN 107, VAL 108, GLN 110, THR 111, GLN-127, LYS 137, GLY 138, ASN 151, ILE 152, ASP 153, SER 158, THR 292, PHE 294, and ASP 295.[44] Many of these interactions were similar to those observed in this study. Shehzadi et al[45] also reported hydrophobic interactions between nonanoic acid and methyl ester, methanolic extracts of *Jacquemontii* Blume and several amino acids, including PHE 294, THR 111, ASN 151, ILE 106, VAL 104, ARG 105, and ASP 295. These amino acids were significantly responsible for the docking scores reported in this

COMPOUNDS		INTERACTING AMINO ACIDS
HB	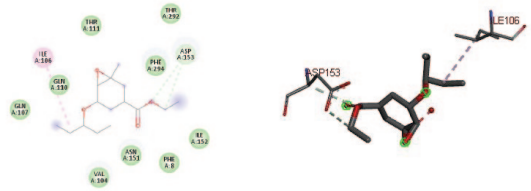	ILE106, ASP 153
HC	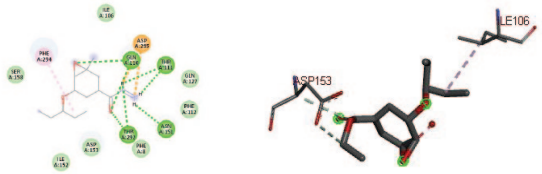	GLN 110, THR111, ASN151, THR292, PHE294
HD	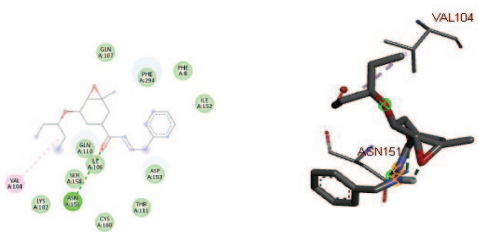	ASN151, VAL 104
HE	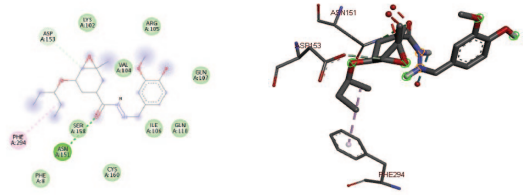	ASN151, ASP153, PHE 294
HF	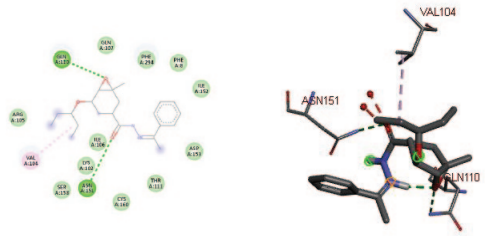	GLN 110, VAL104, ASN151
HG	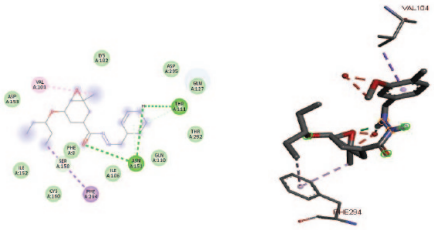	PHE 294, VAL104, ASN 151, THR111
HH	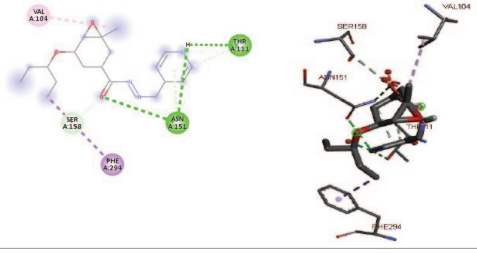	SER 158, VAL 104, THR 111, ASN 151, PHE 294

Figure 4. *(Conitnued)*

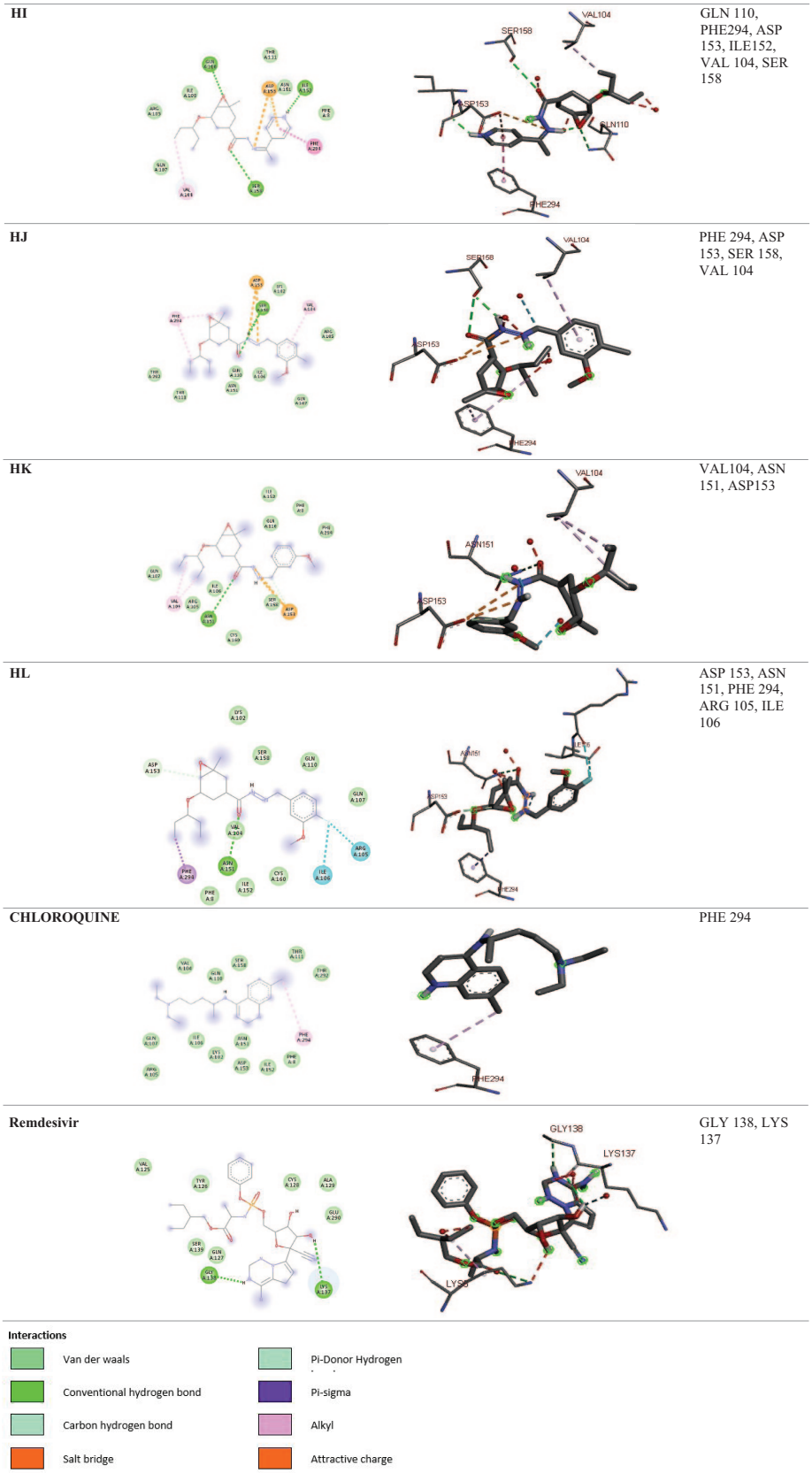

Figure 4. Interaction diagrams of amino acid residues of 6LU7and (1S,5S)-ethyl 1-methyl-5-(pentan-3-yloxy)-7-oxabicyclo[4.1.0]hept-3-ene-3-carboxylate (HB), (1S,5S)-ethyl 1-methyl-5-(pentan-3-yloxy)-7-oxabicyclo[4.1.0]hept-3-ene-3-carboxhydrazide (HC), corresponding hydrazones (HD-HL), chloroquine, and remdesivir.

study. In terms of inhibitory potential against SARS-Cov-2 protease, HC demonstrated a better docking score than a hydrazone-pyridine compound named 3-chloro-2-{(2E)-2-[1-(4chloro phenyl)ethylidene]hydrazinyl}pyridine (-6.4).[46] Furthermore, all of the compounds, except for HB, had better docking scores than remdesivir and chloroquine, frontline drug candidates for combating COVID-19.

Quantum chemical calculations

The HOMO (highest occupied molecular orbital) and LUMO (lowest unoccupied molecular orbital), otherwise known as frontier orbitals in the frontier molecular orbital theory, are the most important orbitals in a molecule. They determine the mode of interaction between a molecule with other species. In addition to this, they provide information on the reactivity as well as stability of specific regions of the molecule. Figure 5 shows the HOMO and LUMO of the compounds (HB – HL). The blue and red regions indicates regions of electron density. Specifically the blue represents positive values of the orbitals, whereas the red region represents negative values of the orbitals.[47] The blue regions in DFT studies represent areas of high electron density, which are important for studying molecular binding and interactions in drug discovery. Positive-valued orbitals indicate electron-rich sites that can facilitate favourable electrostatic interactions like hydrogen bonding or ionic interactions, influencing binding affinity and drug potency. Conversely, the red regions correspond to negative-valued orbitals, which inform about areas of lower electron density. These regions are relevant for studying hydrophobic interactions and can indicate potential binding pockets in the target protein, impacting nonpolar interactions, lipophilicity, and membrane permeability of drug candidates.[48,49] By considering the positive and negative values of orbitals in DFT studies, drug discovery researchers can gain insights into the electronic properties of drug molecules and their interactions with target proteins. This information can help in rational drug design, lead optimization, and predicting the pharmacological activity and potency of potential drug candidates.

In terms of molecular orbital energies, E_{HOMO} is the highest occupied orbital energy and E_{LUMO} is the lowest unoccupied orbital energy. The band gap (E_g) is the name given to the difference between the HOMO and LUMO. E_{HOMO} is frequently linked to a molecule's ability to donate electrons, whereas E_{LUMO} is linked to a molecule's ability to accept electrons. When predicting the chemical reactivity and stability of molecules, the energy gap (E_g) is crucial. Molecules with large E_g are often associated with high chemical stability and low reactivity while molecules with low E_g are associated with low chemical stability and high chemical reactivity.[50] The energy gap of the molecules in this study followed the following order: HC > HB > HF > HI > HD > HL > HG > HH > HK > HE > HJ. Ionization energy (I) is an important chemical parameter. It refers to the amount of energy required to eject an electron from a molecule. High ionization energy correlates with low reactivity and high chemical inertness, while low ionization energy correlates with high reactivity and low chemical inertness.[51] The ionization energy of the compounds follows the same trend as the energy gap.

Chemical hardness (η) refers to the resistance of a molecule to exchange electron density with the environment.[38] Molecules with high chemical hardness often called hard molecules possess large energy gaps while molecules with low chemical hardness possess low energy gaps. According to Table 2, HC is the hardest molecule, and it possesses the lowest softness while HJ is the least hard. The chemical hardness of the molecules follows the trend: HC > HB > HF > HI > HD > HL > HG > HH > HK > HE > HJ.

On the contrary, electronic chemical potential (μ) describes the change in a molecule's energy with regard to the amount of electrons at a certain potential.[38] It is associated with another reactivity descriptor known as the electrophilicity index (ω).[38] The energy stability of a molecule following the acquisition of additional electron density from the environment is quantified by the electrophilicity index.[39] While weak electrophiles have low electronic chemical potential and large chemical hardness, strong electrophiles have high electronic chemical potential and low chemical hardness.[38] All the compounds had electrophilicity index values higher than 0.8; hence, they are likely to act as strong electrophiles and display high interaction affinity, which may result in increased potential to serve as drug candidates.[52]

The MESP is useful for predicting a molecule's chemical reactivity. It provides a visual expression of the shape, size, and potential of the molecules by employing a grading system as a plot of electrostatic potential (ESP) over electron density.[53] It predicts the reactive sites of molecules by providing information on their nucleophilic and electrophilic regions. Interpretation of MESP results can provide valuable information. For example, regions with negative ESP typically indicate areas of high electron density, suggesting nucleophilic sites capable of participating in chemical reactions. Positive ESP regions, on the contrary, often correspond to electrophilic sites where electrons are more likely to be attracted, indicating potential reaction sites. Furthermore, the analysis of the MESPs of compounds can help in understanding molecular interactions, such as hydrogen bonding, pi-stacking, or electrostatic interactions between molecules. By comparing the ESP distributions of different molecules, researchers can predict the likelihood and strength of intermolecular interaction.[54]

In the compounds' MESP analysis, the resulting ESP maps exhibited regions with negative ESP, typically depicted as red, and regions with positive ESP, often represented as blue. These colours help visualize the distribution of electron density and the charge distribution within the molecules. As a result, the

Compounds	HOMO	LUMO
HB	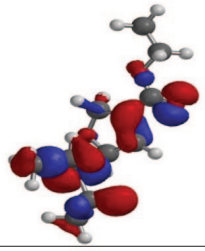	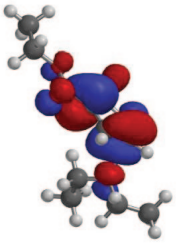
HC	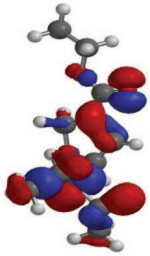	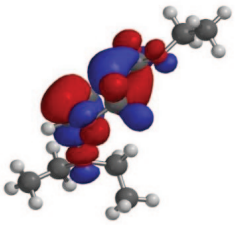
HD	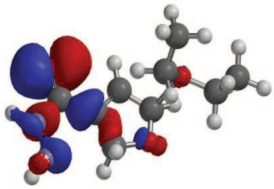	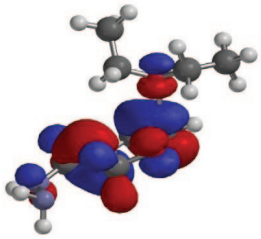
HE	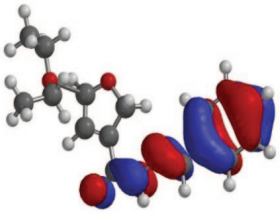	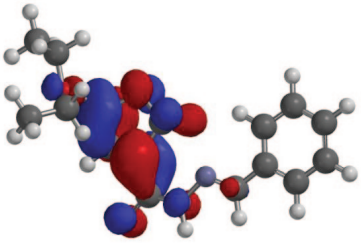
HF	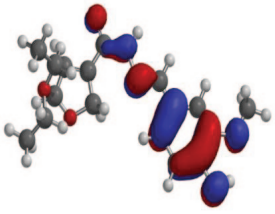	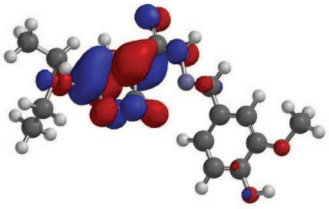
HG	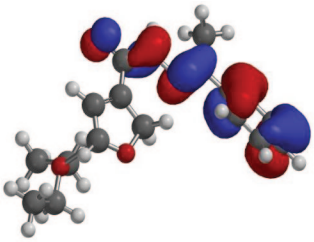	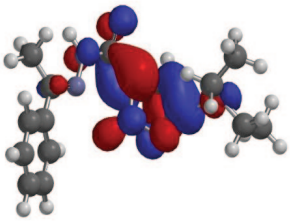

Figure 5. *(Conitnued)*

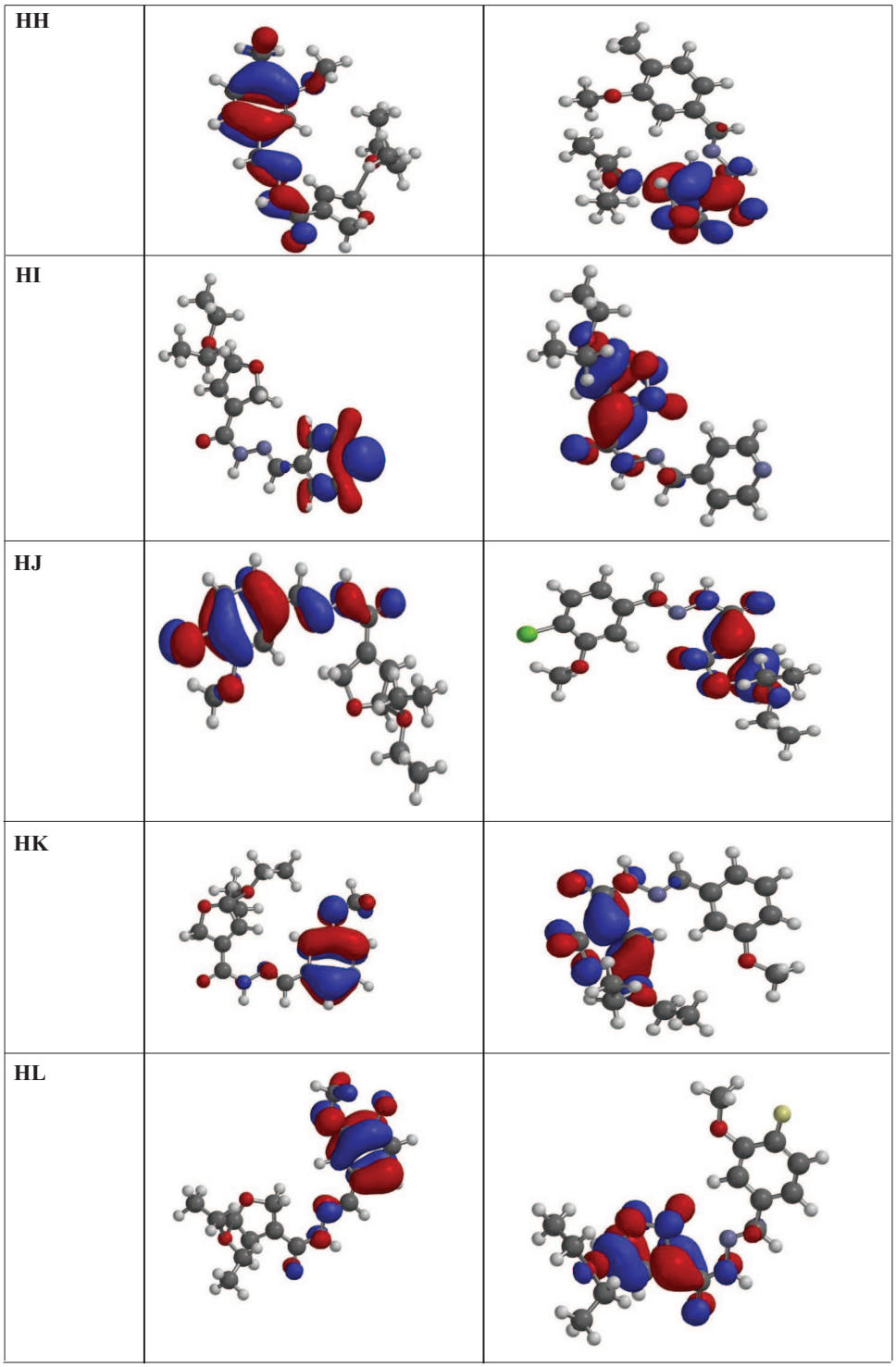

Figure 5. (HOMO and LUMO) of (1S,5S)-ethyl 1-methyl-5-(pentan-3-yloxy)-7-oxabicyclo[4.1.0]hept-3-ene-3-carboxylate (HB), (1S,5S)-ethyl 1-methyl-5-(pentan-3-yloxy)-7-oxabicyclo[4.1.0]hept-3-ene-3-carboxhydrazide (HC) and corresponding hydrazones (HD-HL). HOMO indicates highest occupied molecular orbital; LUMO, lowest unoccupied molecular orbital.

blue regions are likely to be centres for nucleophilic attack whereas the red regions are likely to be centres for electrophilic attack.[55] Oxygen-containing regions within the compounds were shown to be electron-rich regions. As a result, they are susceptible to hydrogen bonding interactions and electrophilic attacks. While aromatic regions and alkyl groups were reported to be electron deficient and susceptible to nucleophilic attack. Figure 6 shows the MESP of the compounds. The MESP analysis of the compounds aligns with the docking results, revealing the presence of oxygen-containing electron-rich regions that form hydrogen bonding interactions with specific protein residues. This observation is supported by

Table 2. Quantum parameters of the compounds.

COMPOUNDS	E_{HOMO} (EV)	E_{LUMO} (EV)	E_G (EV)	η (EV)	χ (EV)	μ (EV)	I (EV)	A (EV)	ω (EV)
HB	−6.67	−1.07	5.60	2.80	−2.80	−3.87	6.67	1.07	2.67
HC	−6.72	−0.90	5.82	2.91	−2.91	−3.81	6.72	0.90	2.49
HD	−6.20	−1.43	4.77	2.39	−2.39	−3.82	6.20	1.43	3.05
HE	−5.75	−1.32	4.43	2.22	−2.22	−3.54	5.75	1.32	2.82
HF	−6.19	−1.11	5.08	2.54	−2.54	−3.65	6.19	1.11	2.62
HG	−6.03	−1.34	4.69	2.35	−2.35	−3.69	6.03	1.34	2.90
HH	−6.59	−1.91	4.68	2.34	−2.34	−4.25	6.59	1.91	3.86
HI	−6.44	−1.57	4.87	2.44	−2.44	−4.01	6.44	1.57	3.29
HJ	−5.96	−1.64	4.32	2.16	−2.16	−3.80	5.96	1.64	3.34
HK	−6.07	−1.42	4.65	2.33	−2.33	−3.75	6.07	1.42	3.02
HL	−6.13	−1.40	4.73	2.37	−2.37	−3.77	6.13	1.40	3.00

Abbreviations: E_{HOMO}, highest occupied molecular orbital energy; E_{LUMO}, lowest unoccupied molecular orbital energy.

Figure 6. MESP of (1S,5S)-ethyl 1-methyl-5-(pentan-3-yloxy)-7-oxabicyclo[4.1.0]hept-3-ene-3-carboxylate (HB), (1S,5S)-ethyl 1-methyl-5-(pentan-3-yloxy)-7-oxabicyclo[4.1.0]hept-3-ene-3-carboxhydrazide (HC) and corresponding hydrazones (HD-HL). MESP indicates molecular electrostatic potential.

the interaction diagrams, which illustrate the formation of hydrogen bonds between the compounds and the identified protein residues.

Drug-likeness

The drug-likeness results as shown in Table 3 revealed that the 11 compounds displayed acceptable drug-like properties as none of them violated Lipinski's and Veber's rule. The

Table 3. Drug-likeness parameters of compounds.

COMPOUNDS	FORMULA	MW	#ROTATABLE BONDS	#H-BOND ACCEPTORS	#H-BOND DONORS	TPSA	MLOGP	GI ABSORPTION
HB	$C_{15}H_{24}O4$	268.35	7	4	0	48.06	1.71	High
HC	$C_{13}H_{22}N_2O_3$	254.33	6	4	2	76.88	0.77	High
HD	$C_{20}H_{26}N_2O_3$	342.43	8	4	1	63.22	2.12	High
HE	$C_{21}H_{28}N_2O_5$	388.46	9	6	2	92.68	1.27	High
HF	$C_{21}H_{28}N_2O_3$	356.46	8	4	1	63.22	2.35	High
HG	$C_{22}H_{30}N_2O_4$	386.48	9	5	1	72.45	2.02	High
HH	$C_{19}H_{25}N_3O_3$	343.42	8	5	1	76.11	1.08	High
HI	$C_{20}H_{27}N_3O_3$	357.45	8	5	1	76.11	1.31	High
HJ	$C_{21}H_{29}ClN_2O_4$	408.92	9	5	1	72.45	2.37	High
HK	$C_{21}H_{28}N_2O_4$	372.46	9	5	1	72.45	1.8	High
HL	$C_{21}H_{27}FN_2O_4$	390.45	9	6	1	72.45	2.18	High

Abbreviation: GI, Gastrointestinal ; MLOGP, Molecular logarithm of the partition coefficient; MW, Molecular weight; TPSA, Topological polar surface area.

Lipinski rule of 5 states that drugs that do not violate one of the following properties were likely to be potential oral drug candidates. These properties include molecular weight ⩽ 500 Daltons, log p ⩽ 5, hydrogen bond acceptors ⩽ 10 and hydrogen bond acceptors donors ⩽5.[14,56] In addition, none of the compounds violated the Vebers rule, which is used to predict the oral bioavailability of a drug. The Vebers rule states that compounds with polar surface area ⩽ 140, hydrogen bonds ⩽ 12, and rotatable bonds ⩽ 10 are likely to exhibit oral bioavailability.[57] Gastrointestinal (GI) absorption is associated with the ability of a potential of a drug candidate to be transported into the gastrointestinal tract of an individual.[58] The results revealed that all the compounds displayed high gastrointestinal absorption. The drug-likeness results strongly suggest that the compounds are potential candidates for the inhibition of COVID-19 main protease.

Conclusion

The DFT results reveal the electronic properties of the compounds. The energy gap, electronic chemical potential, chemical hardness, ionization potential, electronegativity and electrophilicity index computed showed that the compounds were strong electrophiles. The docking results revealed that the oseltamivir intermediate-based hydrazones showed better interaction with the main protease derived from the coronavirus. They showed higher docking scores than the frontline drugs employed in the treatment of coronavirus: chloroquine and remdesivir. The drug-likeness results reveal that the compounds were potential drug candidates as none of them violated Vebers and Lipinski's rule. Hence, they qualify as potential inhibitors of COVID-19 main protease.

Author Contributions

OFA contributed to conceptualization, supervision, investigation, methodology, validation, data curation, writing – review & editing. EGF contributed to supervision, investigation, methodology, validation, data curation, writing – original draft, review & editing. OOA contributed to Data acquisition, methodology, writing – review & editing. SCC contributed to Methodology, data curation, writing – original draft.

REFERENCES

1. WHO coronavirus (COVID-19) dashboard. https://covid19.who.int. Accessed April 3, 2023.
2. Hagar M, Ahmed HA, Aljohani G, Alhaddad OA. Investigation of some antiviral N-heterocycles as COVID 19 drug: molecular docking and DFT calculations. *Int J Mol Sci*. 2020;21:3922.
3. Chhetri BK, Tedbury PR, Sweeney-Jones AM, et al. Marine natural products as leads against SARS-CoV-2 infection. *J Nat Prod*. 2022;85:657-665.
4. Reiner Ž, Hatamipour M, Banach M, et al. Statins and the COVID-19 main protease: in silico evidence on direct interaction. *Arch Med Sci*. 2020;16:490-496.
5. Ghasemi L, Esfahani MH, Abbasi A, Behzad M. Synthesis and crystal structures of new mixed-ligand schiff base complexes containing N-donor heterocyclic co-ligands: Molecular docking and pharmacophore modeling studies on the main proteases of SARS-CoV-2 virus (COVID-19 disease). *Polyhedron*. 2022;220:115825.
6. Hu Y, Lewandowski EM, Tan H, et al. Naturally occurring mutations of SARS-CoV-2 main protease confer drug resistance to nirmatrelvir [published online ahead of print September 6, 2022]. *bioRxiv*. doi:10.1101/2022.06.28.497978.
7. Vuong W, Khan MB, Fischer C, et al. Feline coronavirus drug inhibits the main protease of SARS-CoV-2 and blocks virus replication. *Nat Commun*. 2020;11:4282.
8. Choudhury C. Fragment tailoring strategy to design novel chemical entities as potential binders of novel corona virus main protease. *J Biomol Struct Dyn*. 2021;39:3733-3746.
9. Adem S, Eyupoglu V, Sarfraz I, Rasul A, Ali M. Identification of potent COVID-19 main protease (Mpro) inhibitors from natural polyphenols: an in silico strategy unveils a hope against CORONA. 2020. https://www.preprints.org/manuscript/202003.0333/v1.
10. Cui W, Yang K, Yang H. Recent progress in the drug development targeting SARS-CoV-2 main protease as treatment for COVID-19. *Front Mol Biosci*. 2020;7:616341.

11. Wu Y, Li Z, Zhao YS, Huang YY, Jiang MY, Luo HB. Therapeutic targets and potential agents for the treatment of COVID-19. *Med Res Rev*. 2021;41:1775-1797.
12. Adeboye OO, Agboluaje SA, Akinyele OF. Molecular docking studies of inhibitory activities of Phytochemicals in Calotropis procera against α-glucosidase hydrolase Sus B. *J Chem Soc Niger*. 2021;46. https://journals.chemsociety.org.ng/index.php/jcsn/article/view/599.
13. Mermer A, Bayrak H, Alyar S, Alagumuthu M. Synthesis, DFT calculations, biological investigation, molecular docking studies of β-lactam derivatives. *J Mol Struct*. 2020;1208:127891.
14. Akinyele OF, Fakola EG, Oyeneyin O, et al. Molecular docking study of primaquine-favipiravir based compounds as potential inhibitors of COVID-19 main protease. *Eur Rev Chem Res*. 2020;7:3-15. doi:10.13187/ercr.2020.1.3.
15. Yalcin S. Molecular docking, drug likeness, and ADMET analyses of passiflora compounds as P-glycoprotein (P-gp) inhibitor for the treatment of cancer. *Curr Pharmacol Rep*. 2020;6:429-440.
16. Chen X, Leng J, Rakesh KP, et al. Synthesis and molecular docking studies of xanthone attached amino acids as potential antimicrobial and anti-inflammatory agents. *Medchemcomm*. 2017;8:1706-1719.
17. Olanrewaju AA, Ibeji CU, Oyeneyin OE. Biological evaluation and molecular docking of some newly synthesized 3d-series metal (II) mixed-ligand complexes of fluoro-naphthyl diketone and dithiocarbamate. *SN Appl Sci*. 2020;2:678.
18. Metibemu DS, Oyeneyin OE, Omotoyinbo DE, et al. Molecular docking and quantitative structure activity relationship for the identification of novel phyto-inhibitors of matrix metalloproteinase-2. *Sci Lett*. 2020;8:61-68.
19. Akinyele OF, Odiaka TI, Adejoro IA. Structural and DFT studies on molecular structure of pyridino-1-4-η-cyclohexa-1,3-diene and 2-methoxycyclohexa-1,3-diene irontricarbonyl complexes. *Am J Phys Chem*. 2019;8:41. doi:10.11648/j.ajpc.20190802.12.
20. Ejalonibu MA, Elrashedy AA, Lawal MM, et al. Dual targeting approach for Mycobacterium tuberculosis drug discovery: insights from DFT calculations and molecular dynamics simulations. *Struct Chem*. 2020;31:557-571.
21. Sabe VT, Ntombela T, Jhamba LA, et al. Current trends in computer aided drug design and a highlight of drugs discovered via computational techniques: a review. *Eur J Med Chem*. 2021;224:113705.
22. Shakdofa MM, Shtaiwi MH, Morsy N, Abdel-rassel T. Metal complexes of hydrazones and their biological, analytical and catalytic applications: a review. *Main Group Chem*. 2014;13:187-218.
23. Avaji PG, Kumar CH, Patil SA, Shivananda KN, Nagaraju C. Synthesis, spectral characterization, in-vitro microbiological evaluation and cytotoxic activities of novel macrocyclic bis hydrazone. *Eur J Med Chem*. 2009;44:3552-3559.
24. Kalia J, Raines RT. Hydrolytic stability of hydrazones and oximes. *Angew Chem Int Ed Engl*. 2008;47:7523-7526.
25. Akinyele OF, Alimi IA. Quantitative structural activity relationship of hydrazide derivatives of loratadine: a combined density functional theory and in silico study. *J Chem Soc Niger*. 2019;44. https://journals.chemsociety.org.ng/index.php/jcsn/article/view/341.
26. De Oliveira Carneiro Brum J, França TCC, LaPlante SR, Villar JDF. Synthesis and biological activity of hydrazones and derivatives: a review. *Mini Rev Med Chem*. 2020;20:342-368.
27. Tan Q, Duan L, Ma Y, et al. Is oseltamivir suitable for fighting against COVID-19: in silico assessment, in vitro and retrospective study. *Bioorg Chem*. 2020;104:104257.
28. Abu-Melha S, Edrees MM, Riyadh SM, Abdelaziz MR, Elfiky AA, Gomha SM. Clean grinding technique: a facile synthesis and in silico antiviral activity of hydrazones, pyrazoles, and pyrazines bearing thiazole moiety against SARS-CoV-2 main protease (Mpro). *Molecules*. 2020;25:4565.
29. Tabbiche A, Bouchama A, Chafai N, et al. New bis hydrazone: synthesis, X-ray crystal structure, DFT computations, conformational study and in silico study of the inhibition activity of SARS-CoV-2. *J Mol Struct*. 2022;1261:132865.
30. Sharma PC, Sharma D, Sharma A, et al. Hydrazone comprising compounds as promising anti-infective agents: chemistry and structure-property relationship. *Mater Today Chem*. 2020;18:100349.
31. Mphahlele MJ, Agbo EN, Gildenhuys S, Setshedi IB. Exploring biological activity of 4-oxo-4 H-furo [2, 3-h] chromene derivatives as potential multi-target-directed ligands inhibiting cholinesterases, β-secretase, cyclooxygenase-2, and lipoxygenase-5/15. *Biomolecules*. 2019;9:736.
32. Tao K, Tzou PL, Nouhin J, et al. The biological and clinical significance of emerging SARS-CoV-2 variants. *Nat Rev Genet*. 2021;22:757-773.
33. Lauring AS, Malani PN. Variants of SARS-CoV-2. *JAMA*. 2021;326:880-880.
34. Wahbeh J, Milkowski S. The use of hydrazones for biomedical applications. *SLAS Technol*. 2019;24:161-168.
35. Das B, Baidya AT, Mathew AT, Yadav AK, Kumar R. Structural modification aimed for improving solubility of lead compounds in early phase drug discovery. *Bioorg Med Chem*. 2022;56:116614.
36. Alshetaili AS, Ansari MJ, Anwer MK, et al. Enhanced oral bioavailability of ibrutinib encapsulated poly (lactic-co-glycolic acid) nanoparticles: pharmacokinetic evaluation in rats. *Curr Pharm Anal*. 2019;15:661-668.
37. Ishabiyi FO, Ogidi J, Olukade BA, et al. Computational evaluation of Azadirachta Indica-derived bioactive compounds as potential inhibitors of NLRP3 in the treatment of Alzheimer's disease [published online ahead of print January 18, 2023]. *J Alzheimers Dis*. doi:10.3233/JAD-221020.
38. Domingo LR, Ríos-Gutiérrez M, Pérez P. Applications of the conceptual density functional theory indices to organic chemistry reactivity. *Molecules*. 2016;21:748.
39. Ayeni AO, Akinyele OF, Hosten EC, et al. Synthesis, crystal structure, experimental and theoretical studies of corrosion inhibition of 2-((4-(2-hydroxy-4-methylbenzyl) piperazin-1-yl) methyl)-5-methylphenol – a Mannich base. *J Mol Struct*. 2020;1219:128539.
40. Awotuya IO, Fakola EG, Olusola AJ, et al. Exploring the protein tyrosine phosphatase 1B inhibitory potentials of naturally occurring Brazilin-type homoisoflavonoids: a computational approach. *Chem Africa*. 2022;5:1493-1502.
41. Adane L, Bhagat S, Arfeen M, et al. Design and synthesis of guanylthiourea derivatives as potential inhibitors of Plasmodium falciparum dihydrofolate reductase enzyme. *Bioorg Med Chem Lett*. 2014;24:613-617.
42. Delgadillo-Armendariz NL, Rangel-Vázquez NA, Márquez-Brazón EA. Determination of structural properties in the adsorption of drugs on chitosan-hydrogels for type 2 diabetes by means of the PM6 method. *Rev Colomb Quím*. 2020;49:12-17.
43. Ibrahim A, Ipinloju N, Atasie NH, Babalola RM, Muhammad SA, Oyeneyin OE. Discovery of small molecule PARKIN activator from antipsychotic/anti-neuropsychiatric drugs as therapeutics for PD: an in silico repurposing approach [published online ahead of print February 3, 2023]. *Appl Biochem Biotechnol*. doi:10.1007/s12010-023-04376-2.
44. Indu P, Rameshkumar MR, Arunagirinathan N, Al-Dhabi NA, Valan Arasu M, Ignacimuthu S. Raltegravir, indinavir, tipranavir, dolutegravir, and etravirine against main protease and RNA-dependent RNA polymerase of SARS-CoV-2: a molecular docking and drug repurposing approach. *J Infect Public Health*. 2020;13:1856-1861.
45. Shehzadi S, Khan SM, Mustafa G, et al. Antiviral COVID-19 protein and molecular docking: in silico characterization of various antiviral compounds extracted from Arisaema jacquemontii Blume. *Front Public Health*. 2022;10:964741.
46. Topal T, Zorlu Y, Karapınar N. Synthesis, X-ray crystal structure, IR and Raman spectroscopic analysis, quantum chemical computational and molecular docking studies on hydrazone-pyridine compound: as an insight into the inhibitor capacity of main protease of SARS-CoV2. *J Mol Struct*. 2021;1239:130514.
47. Ucak-Astarlioglu M, Edwards S, Zoto CA. Spectroscopic properties of two conjugated organic dyes: a computational and experimental study. *J Lab Chem Educ*. 2017;5:32-39.
48. Saba A, Muhammad S, Khera RA, et al. Identification of halogen-based derivatives as potent inhibitors of estrogen receptor alpha of breast cancer: an in-silico investigation. *J Comput Biophys Chem*. 2022;21:181-205.
49. Gadre SR, Suresh CH, Mohan N. Electrostatic potential topology for probing molecular structure, bonding and reactivity. *Molecules*. 2021;26:3289.
50. Obi-Egbedi NO, Essien KE, Obot IB, Ebenso EE. 1, 2-Diaminoanthraquinone as corrosion inhibitor for mild steel in hydrochloric acid: weight loss and quantum chemical study. *Int J Electrochem Sci*. 2011;6:913-930.
51. Oyeneyin OE, Ojo ND, Ipinloju N, James AC, Agbaffa EB. Investigation of corrosion inhibition potentials of some aminopyridine schiff bases using density functional theory and Monte Carlo simulation. *Chem Africa*. 2022;5:319-332.
52. Kulandaisamy A, Panneerselvam M, Solomon RV, et al. Halogen-based 17β-HSD1 inhibitors: insights from DFT, docking, and molecular dynamics simulation studies. *Molecules*. 2022;27:3962.
53. Stefaniu A, Pintilie L. Molecular descriptors and properties of organic molecules. In: Akitsu T, ed. *Symmetry (Group Theory) and Mathematical Treatment in Chemistry*. Rijeka, Croatia: IntechOpen; 2018:161-176.
54. Fatima A, Pooja K, Savita S, et al. Quantum chemical, experimental spectroscopic, Hirshfeld surface and molecular docking studies of the anti-microbial drug Sulfathiazole. *J Mol Struct*. 2021;1245:131118.
55. Faloye KO, Bekono BD, Fakola EG, et al. Elucidating the glucokinase activating potentials of naturally occurring prenylated flavonoids: an explicit computational approach. *Molecules*. 2021;26:7211.
56. Lipinski CA, Lombardo F, Dominy BW, Feeney PJ. Experimental and computational approaches to estimate solubility and permeability in drug discovery and development settings. *Adv Drug Deliv Rev*. 1997;23:3-25.
57. Veber DF, Johnson SR, Cheng HY, Smith BR, Ward KW, Kopple KD. Molecular properties that influence the oral bioavailability of drug candidates. *J Med Chem*. 2002;45:2615-2623.
58. Wang NN, Huang C, Dong J, et al. Predicting human intestinal absorption with modified random forest approach: a comprehensive evaluation of molecular representation, unbalanced data, and applicability domain issues. *RSC Adv*. 2017;7:19007-19018.